

Design, Synthesis, and Evaluation of Novel Biarylpyrimidines: A New Class of Ligand for Unusual Nucleic Acid Structures

Richard T. Wheelhouse,*[†] Sharon A. Jennings,[†] Victoria A. Phillips,[†] Dimitrios Pletsas,[†] Peter M. Murphy,[†] Nichola C. Garbett,[‡] Jonathan B. Chaires,[‡] and Terence C. Jenkins[§]

School of Pharmacy, University of Bradford, Bradford, West Yorkshire BD7 1DP, U.K., James Graham Brown Cancer Center, University of Louisville, Louisville, Kentucky 40202, and Morvus Technology Limited, Building 115, Porton Down Science Park, Salisbury, Wiltshire SP4 0JQ, U.K.

Received March 20, 2006

Biarylpyrimidines are characterized as selective ligands for higher-order nucleic acid structures. A concise and efficient synthesis has been devised incorporating Suzuki biaryl cross-coupling of dihalopyrimidines. Two ligand series are described based on the parent thioether 4,6-bis[4-[[2-(dimethylamino)ethyl]mercapto]phenyl]pyrimidine (**1a**) and amide 4,6-bis(4[[2-(dimethylamino)ethyl]carboxamido]phenyl)pyrimidine (**2a**) compounds. In UV thermal denaturation studies with the poly(dA)•[poly(dT)]₂ triplex structure, thioethers showed stabilization of the triplex form ($\Delta T_m \leq 20$ °C). In contrast, amides showed duplex stabilization ($\Delta T_m \leq 15$ °C) and either negligible stabilization or specific destabilization ($\Delta T_m = -5$ °C) of the triplex structure. Full spectra of nucleic acid binding preferences were determined by competition dialysis. The strongest interacting thioether bound preferentially to the poly(dA)•[poly(dT)]₂ triplex, $K_{app} = 1.6 \times 10^5$ M⁻¹ ($40 \times K_{app}$ for CT DNA duplex). In contrast, the strongest binding amide selected the (T₂G₂₀T₂)₄ quadruplex structure, $K_{app} = 0.31 \times 10^5$ M⁻¹ ($6.5 \times K_{app}$ for CT DNA duplex).

Introduction

Following the completion of the human genome project and its conclusion that a relatively small number (30 000) of genes “encode” a human being, it now appears that the definition and functional control of the whole organism are determined not by the simple on/off expression of genes but by the dynamic interplay of gene expression over time.¹ This offers the prospect of a fundamentally new medicine based on regulating gene activity rather than altering the behavior of proteins. The targets for drug design will be nucleic acids: not only B-form DNA sequences but also specific and unusual structures, such as the high-order DNA triplexes and quadruplexes (tetraplexes),^{2–4} DNA•RNA hybrids,⁵ and specific RNA secondary structures.⁶ A tantalizing glimpse of this new chemotherapy is seen from evidence that (i) the c-myc oncogene promoter sequence includes a G-rich tract that is able to adopt a quadruplex structure⁷ and (ii) treatment of tumor cells with a quadruplex DNA-binding ligand alters the expression of both this oncogene and other genes under its control.⁸ Moreover, putative quadruplex-forming sequences appear to be common in the promoter regions of growth control genes.^{9–16}

Ligands with precisely defined selectivity for nucleic acid structure therefore have a range of potential therapeutic applications, while the need to avoid undesirable cytotoxic effects dictates that competing affinity for duplex structures must be eliminated in any design program.¹⁷ Herein, we report fully¹⁸ the design and synthesis of biarylpyrimidines and describe investigations of their intriguing and selective binding preferences toward higher-order DNA secondary structures. Structural factors that either direct binding selectivity toward quadruplex and triplex DNA or induce specific triplex destabilization have been identified.

Results and Discussion

Ligand Design. 4,6-Biarylpyrimidine **1a** is planar in its crystal form and known to behave, in part, as a modest duplex DNA intercalator.¹⁹ However, steric crowding inhibits adoption of equivalent planar conformations in the analogous triphenyl ring system. Energy profiles were determined, using semi-empirical molecular modeling, for rotation about one interannular bond of 1,3-diphenylbenzene (“triphenyl”) and a range of substituted biarylpyrimidines (see Supporting Information). In triphenyl, energy maxima occur when the molecule approaches a planar conformation, i.e., torsion angle $\theta = 0^\circ, 180^\circ$, etc. These energy barriers are lowered by 1.1 kcal mol⁻¹ in the analogous biarylpyrimidine system because of relief of steric interactions around the interannular bond by introduction of the two nitrogen atoms in the pyrimidine ring. Such stabilization is largely unaffected by the nature of the para substituent on each of the phenyl rings. Thus, under the influence of an external stacking constraint (e.g., crystal packing or DNA intercalation) the near-planar conformation may become optimal for the unfused tricyclic system.¹⁹

Examination of the crystal structure of biarylpyrimidine **1a** shows the long dimension of the putatively planar, intercalating core portion of the molecule (13.2 Å) to be a closer match to the larger threading distances presented by quadruplex (10.8–13.0 Å)²⁰ or triplex (7.0–12.4 Å)^{21,22} nucleic acid structures rather than to DNA duplexes that offer distances of 5.2–7.3 Å, depending on sequence (Figure 1). It was also envisaged that the potentially planar chromophore could be extended by substitution of amide groups for the thioethers (i.e., **1** → **2**) and to thereby further direct nucleic acid-binding preferences toward higher-order structures. On this basis two distinct series of ligands based on thioether and amide linkages (**1** and **2**, respectively) bearing ω -aminoalkyl side chains were identified for synthesis and further investigation.

Synthesis. To generate a structurally diverse library of compounds, a concise, high-yielding synthetic route was required with the potential for adaptation to solid-phase methods.

* To whom correspondence should be addressed. Phone: +44 (0) 1274 234710. Fax: +44 (0) 1274 235600. E-mail: r.t.wheelhouse@brad.ac.uk.

[†] University of Bradford.

[‡] University of Louisville.

[§] Morvus Technology Limited.

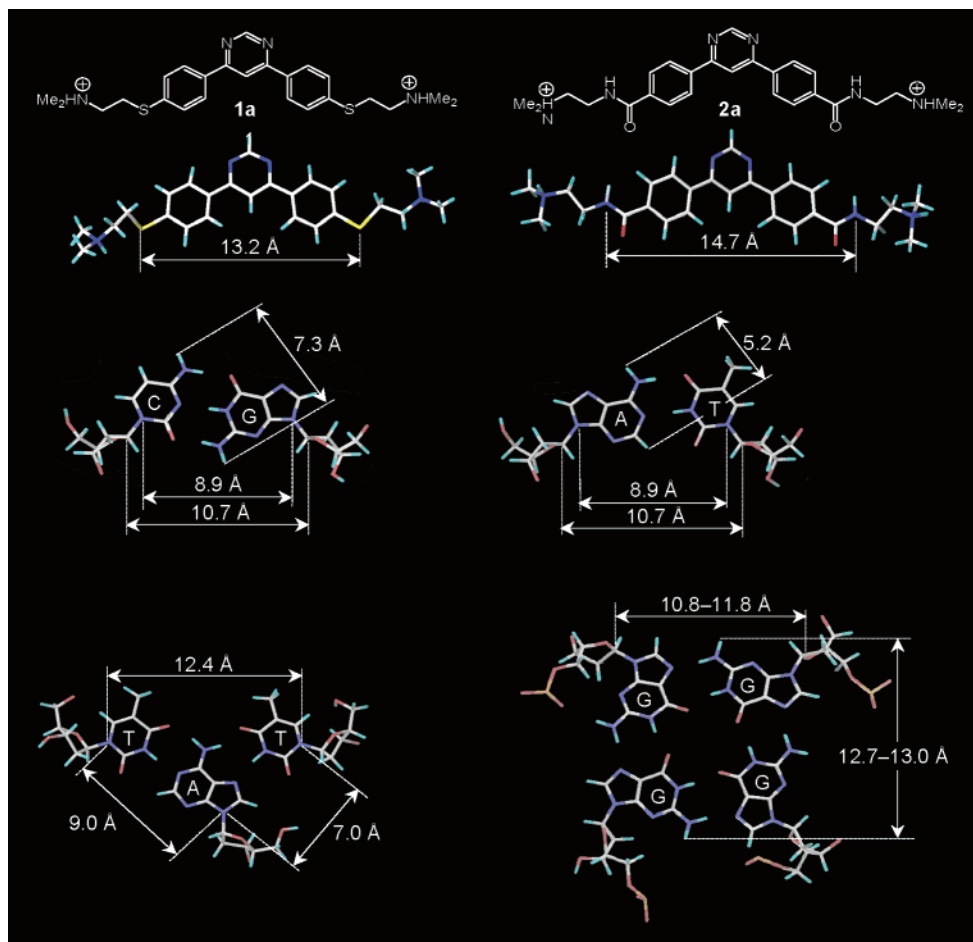
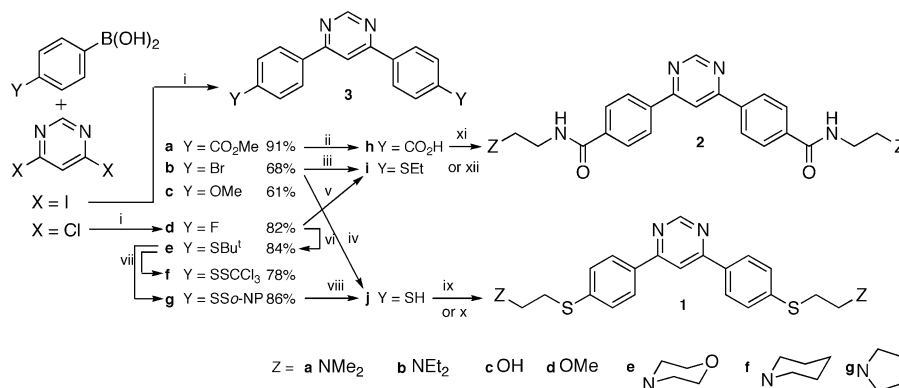


Figure 1. Comparison of the dimensions of thioether **1a** (top, left) and amide **2a** (top, right) with the cross-sections of base plane arrangements in duplex, triplex, and quadruplex DNA structures.

Scheme 1^a



^a Reagents and conditions: (i) Pd(Ph₃P)₄, K₂CO₃, PhMe/EtOH 9:1, Δ , N₂; (ii) NaOH, Δ , then HCl; (iii) NaSEt, DMF, 80 °C, 48 h, 62%; (iv) NaSEt, DMF, Δ , \leq 56%; (v) NaSEt, DMF, room temp, 22h; (vi) NaSBU^t, DMF, 70 °C, 18 h; (vii) RSCl, AcOH, 50 °C, 24 h; (viii) NaBH₄, EtOH/H₂O 100:15, pH 8–9, 30 min, 72%; (ix) Z(CH₂)₂Cl, NaOH, EtOH, \leq 87%, then HBr; (x) Z(CH₂)₂Cl, K₂CO₃, DMF, room temp, \leq 76%, then HBr; (xi) Z(CH₂)₂NH₂, PyBOP, Et₃N, CH₂Cl₂, room temp, then HBr, \leq 70% yield; (xii) Z(CH₂)₂NH₂, Δ , \leq 88%, then HBr.

Biarylpyrimidines have hitherto been prepared either by condensation of 1,3-diketones with formamide^{23,24} or by sequential aryllithium additions to pyrimidine.¹⁹ Previous success with heterocyclic examples of the Suzuki biaryl cross-coupling reaction^{25,26} suggested a superior assembly of the biarylpyrimidine core by Suzuki arylation of a dihalopyrimidine,^{18,27–32} with side chain diversity introduced in subsequent steps. The flexible synthetic protocol is outlined in the Scheme 1. Briefly, 4,6-diiodopyrimidine³³ was reacted with arylboronic acids in the presence of Pd(Ph₃P)₄ to afford substituted biarylpyrimidines **3a–d** directly in up to 90% yield. Since reaction of bromo-

iodoarenes is known to give superior yields in carbocyclic examples of Suzuki reactions, commercially available 4,6-dichloropyrimidine was converted to 4,6-diiodopyrimidine before arylation. However, subsequent experiments showed that in the heterocyclic cases, a chlorine atom positioned ortho to the ring nitrogen was sufficiently activating to give good yields so that conversion to the iodide was not always essential for efficient synthesis.^{31,34}

Access to the thioether-linked ligands **1** was achieved through nucleophilic substitution of appropriate 2-chloroethylamine derivatives by thiophenol **3j**. The 4-halobiarylpyrimidines **3b**

Table 1. ΔT_m Values ($^{\circ}\text{C}$)^a Determined for CT DNA and Poly(dA)·[Poly(dT)]₂ Triplex DNA in the Presence of Biarylpyrimidine Ligands (All Data Are Mean Values \pm 0.1 $^{\circ}\text{C}$)

Compound		CT DNA ^a		poly(dA)·[poly(dT)] ₂ ^b	
number	Z	ΔT_m^c	$\Delta T_m^{20}/\Delta T_m^{80}^d$	ΔT_m^1	ΔT_m^2
		duplex melt		triplex melt	duplex melt
1a	NMe ₂	12.2	1.14	10.5	0.3
1b	NEt ₂	10.1	1.10	20.2	1.2
1c	OH	0.8	2.87	4.0	0.6
1d	OCH ₃	1.3	1.20	1.7	0.2
1e		1.6	1.01	13.9	1.1
1f		9.7	1.24	17.4	2.8
2a	NMe ₂	11.2	1.45	0.7	7.7
2b	NEt ₂	12.5	1.21	5.7	8.1
2c	OH	1.4	1.01	0.8	1.2
2d	OCH ₃	0.1	1.69	0.8	0.8
2e		2.3	2.33	-1.3 ^e	5.1
2f		13.9	1.40	-5.0 ^e	14.2
2g		13.8	1.40	-5.3 ^e	13.7
3c	-	nd	nd	5.7	1.5

^a 50 μM DNA (in base pairs), 20 μM ligand, 10 mM Na₂HPO₄, NaH₂PO₄, 1 mM Na₂EDTA, pH 7.00 \pm 0.01; T_m for CT DNA = 68.3 $^{\circ}\text{C}$. ^b 50 μM triplex (in base triads), 25 μM ligand, 10 mM sodium cacodylate, 300 mM NaCl, 0.1 mM Na₂EDTA, pH 6.00 \pm 0.01; T_m^1 = 54.2 $^{\circ}\text{C}$ (triplex \rightarrow duplex + single strand) and T_m^2 = 76.8 $^{\circ}\text{C}$ (melt to single strands). ^c $\Delta T_m = T_m(\text{DNA} + \text{ligand}) - T_m(\text{DNA})$. ^d $\Delta T_m^{20}/\Delta T_m^{80}$ = ratio of ΔT_m at 20% to ΔT_m at 80% of the normalized absorbance change during melting. ^e Ligand destabilizes the DNA triplex.

and **3d** were good substrates for nucleophilic aryl substitution reactions, the electron-withdrawing substituent effect of the pyrimidine on the phenyl rings being equivalent to that of a nitro group; the observed chemical shifts of the ring protons (δ_{H} = 8.02, 7.67 ppm for **3b**) were thus similar to those of 4-bromonitrobenzene (8.02, 7.66 ppm).³⁵ Although thiophenol **3j** could be obtained by nucleophilic displacement of the bromoarene **3b** by treatment with excess NaSEt,^{18,36,37} reaction conditions for cleavage of the intermediate thioether **3i** were harsh and led to variable isolated yields. Switching to the fluoroarene **3d** gave the anticipated rate enhancements in the nucleophilic substitution reaction (complete consumption by NaSEt in DMF in 22 h at room temperature compared with 48 h at 80 $^{\circ}\text{C}$). However, little reaction was evident on treatment of **3d** with a wide range of sulfur, oxygen, or nitrogen nucleophiles, even in the presence of DBU; good yields were obtained only with sodium alkanethiolates. Significantly, use of the 4-fluoro substrate **3d** facilitated introduction of the *tert*-butylthioether **3e**, for which alternative methods are available to effect cleavage to the thiophenol. Disappointingly, reaction with Br₂ in the presence of acetyl bromide yielded an intractable disulfide polymer rather than the thioacetate,³⁸ even upon addition of DMAP. Cleavage with sulfinyl chlorides efficiently converted the *tert*-butylthioether to the mixed disulfides **3f** and **3g** (78% and 91% yield, respectively).^{39–41} These stable crystalline derivatives were reduced to the free thiophenol **3j** immediately prior to use.

The amide-linked derivatives **2** could be obtained by direct aminolysis of ester **3a**, but greatly improved yields and easier purifications were achieved following hydrolysis to the free acid **3h** and subsequent amide formation. The utility of various activated carboxylic acid equivalents was investigated. Coupling reactions using acid chlorides, TFP esters, DCC, EDC, and CDI

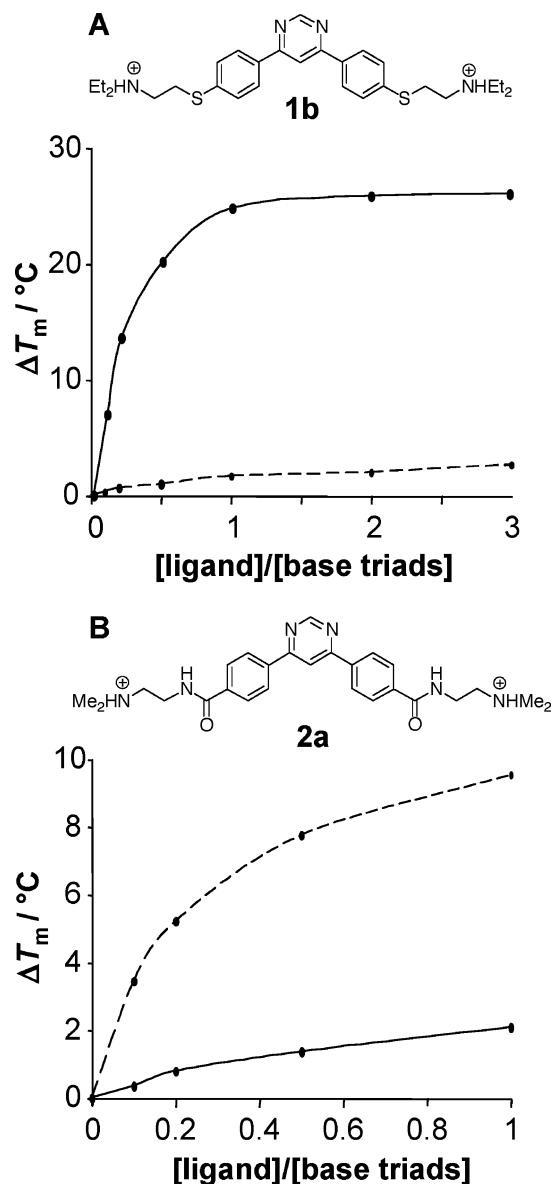


Figure 2. Concentration dependence of melting behaviors of the poly(dA)·[poly(dT)]₂ triplex in the absence and presence of example compounds from the (A) thioether and (B) amide ligand series: (solid lines) ΔT_m^1 (triplex melt \rightarrow duplex + single strand); (dashed lines) ΔT_m^2 (duplex melt \rightarrow single strands). The [ligand]/[DNA] ratio refers to the initial concentrations of each component at low temperatures, using a fixed DNA triplex concentration (50 μM in base triads).

all proved unsuccessful, even with addition of HOBt and NHS to the carbodiimide reactions. High yields were achieved using the peptide-coupling agent PyBOP, where the almost-pure amide precipitate could often be obtained by simple filtration of the reaction mixture. Two series of analogues, thioethers **1a–f** and amides **2a–g**, were prepared. All compounds bearing basic side chains were isolated as their hydrobromide acid addition salts.

UV Spectrophotometric Thermal Melting Studies. Three nucleic acid systems were used for studies of thermal denaturation (melting):^{42,43} calf thymus (CT) DNA, poly(dA)·poly(dT) duplex, and the poly(dA)·[poly(dT)]₂ triplex. Collated ΔT_m data are presented in Figures 2 and 3 and Table 1. In the absence of bound ligands, CT DNA showed a main transition at T_m = 68.3 $^{\circ}\text{C}$. A concentration dependence study indicated that a mole ratio of 50 μM (base pair) CT DNA/20 μM ligand gave \sim 80% maximal stabilization with the parent ligands **1a** and **2a**. All of the cationic ligands examined effected thermal stabilization of

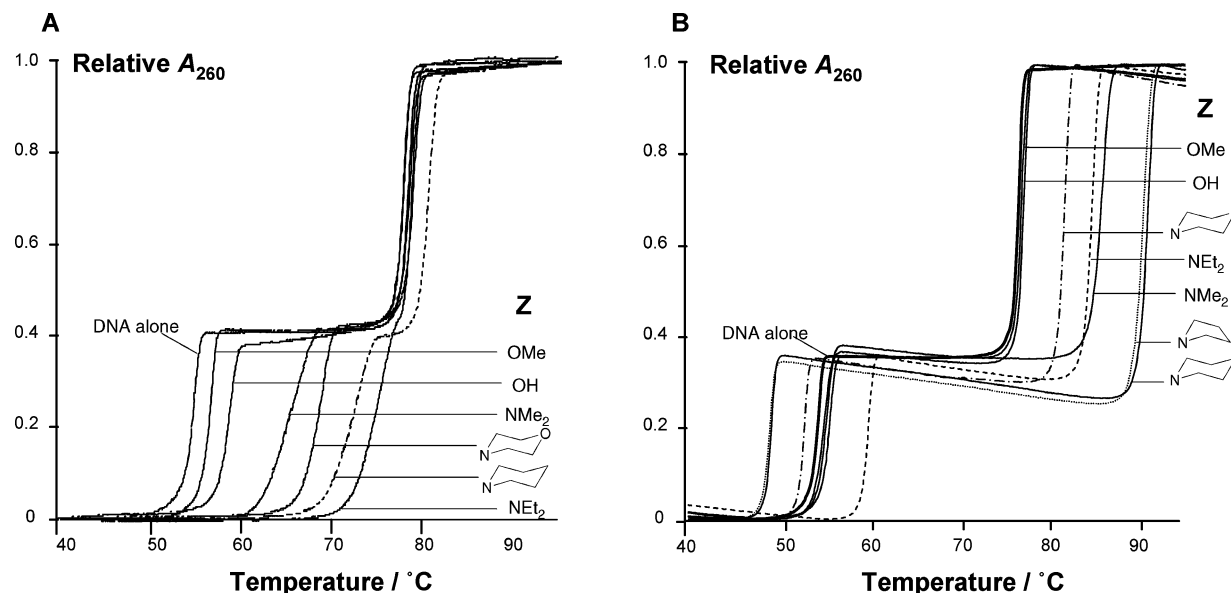


Figure 3. UV melting curves for poly(dA)·[poly(dT)]₂ triplex DNA (fixed at 50 μ M in base triplets) in the absence and presence of (A) thioether ligands **1** or (B) amide ligands **2**. Concentrations: DNA, 50 μ M in base triplets; ligand, 25 μ M. A fixed ligand concentration of 25 μ M was used with optical monitoring at 260 nm.

this DNA duplex, with induced ΔT_m of 10–15 $^{\circ}$ C. The stabilization was independent of the functional group (thioether or amide) linking the core aryl system to the side chain. Furthermore, the shifted curves were not parallel to that obtained for DNA alone and the effect upon the melting profile provides an indicator of sequence binding preference of the ligand. For the normalized A_{260} (i.e., 0–100%) vs temperature curve, the shape of the early part of the melting curve is controlled by A–T base-pair melting; G–C base pairs melt in the higher-temperature range.⁴⁴ A semiquantitative impression of the excess of A–T over G–C stabilization can be obtained by comparing the ΔT_m values at 20% and 80% of the normalized absorbance change during melting (denoted ΔT_m^{20} and ΔT_m^{80} , respectively). This factor is represented by the $\Delta T_m^{20}/\Delta T_m^{80}$ ratio (Table 1). For ligands in both compound series where significant duplex stabilization was shown ($\Delta T_m > 10$ $^{\circ}$ C), the $\Delta T_m^{20}/\Delta T_m^{80}$ parameter was greater than 1.0, indicating preferential stabilization of A–T rich sequences in the CT duplex. This differential behavior was significantly more marked for the amide compounds **2a,b,f,g** ($T_m^{20}/\Delta T_m^{80} = 1.21$ – 1.45) than for the thioethers **1a,b,f** ($T_m^{20}/\Delta T_m^{80} = 1.10$ – 1.24).

The melting curve for poly(dA)·[poly(dT)]₂ triplex DNA in the absence of ligand shows two sequential thermal transitions: $T_m^1 = 54.3$ $^{\circ}$ C (triplex melt \rightarrow duplex + single strand) and $T_m^2 = 77.8$ $^{\circ}$ C (duplex melt \rightarrow all single strands).^{42,43} The effects of examined ligands on the melting behavior of the poly(dA)·[poly(dT)]₂ triplex are shown in Figure 3. The concentration-dependent effects of selected ligands from each series (**1b**, **2a**) on the two melting transitions are shown in Figure 2. Evidence for selective interactions with high-order structures is apparent, with demonstration that the selectivity can be directed by modifying the ligand structure from thioether to amide. Thus, thioether **1b** effected a dramatic and concentration-dependent stabilization of the triplex melting transition up to a maximum $\Delta T_m^1 \approx 24$ $^{\circ}$ C, whereas the duplex melting event was little affected ($\Delta T_m^2 \leq 3$ $^{\circ}$ C). In the case of amide **2a**, the effects on the transitions are reversed and the magnitude of the effects is also much smaller: the triplex to duplex transition is unaffected ($\Delta T_m^1 < 2$ $^{\circ}$ C), while the duplex to single strands melt was increased with a maximum $\Delta T_m^2 \approx 9$ $^{\circ}$ C.

On the basis of concentration dependence studies, a fixed ratio of [ligand]/[base triplets (bt)] of (25 μ M):(50 μ M) was used for comparative analysis of the two ligand series (see Figure 2 and Table 1). Triplex stabilization was common to all thioether ligands bearing ω -amino side chains (**1a,b,f**), demonstrating that the charged ammonium group in the side chain is essential for triplex stabilization. In contrast, the hydroxyethyl (**1c**) and methoxyethyl (**1d**) derivatives showed little evidence for interaction with either triplex- or duplex-form DNA, despite the possibilities for greater hydrogen-bonded DNA–ligand interactions upon binding. The corresponding amides (**2c,d**) showed similarly negligible effects. The extent of triplex stabilization is sensitive to the nature of the basic side chain, with the bulkier and more hydrophobic groups being more effective (e.g., piperidinyll **1f**, $\Delta T_m^1 = 17.4$ $^{\circ}$ C; diethylamino **1b**, $\Delta T_m^1 = 20.2$ $^{\circ}$ C) although there is no apparent correlation with the pK_a of the basic amino group (NMe₂ **1a** < morpholino **1e** < piperidino **1f** < NEt₂ **1b**).

Minor structural alteration to the amides **2** resulted in an entirely different pattern of ΔT_m values (Figure 3B). In general, the simple dialkylamino compounds (e.g., **2a,b**) induced a moderate thermal stabilization of the poly(dA)·poly(dT) duplex ($\Delta T_m^2 \leq 8.1$ $^{\circ}$ C) with little effect on triplex melting ($\Delta T_m^1 \leq 1$ $^{\circ}$ C, except for **2b**). Remarkable structure-selective differences are evident for amide ligands bearing heterocyclic side chains (**2e–g**). Ligands **2f** and **2g** showed closely similar effects, with stabilization of the poly(dA)·poly(dT) duplex ($\Delta T_m^2 \approx 14$ $^{\circ}$ C) and a specific destabilization of the triplex structure ($\Delta T_m^1 \approx -5.3$ $^{\circ}$ C) that preserves the shape of the biphasic melting curve (Figure 3B). This behavior indicates that the ligands show sufficiently high affinity for duplex-form poly(dA)·poly(dT) to competitively displace the third strand from its corresponding DNA triplex structure.

A spectrophotometric titration study showed marked hypochromicity and sharp isosbestic points as poly(dA)·poly(dT) duplex was titrated into a solution containing either thioether **1a** (Figure 4A) or amide **2a** (Figure 4B). The results are consistent with the binding-induced ΔT_m and curve shifts observed with CT DNA. However, a dramatic difference was seen upon addition of poly(dA)·[poly(dT)]₂ triplex to either

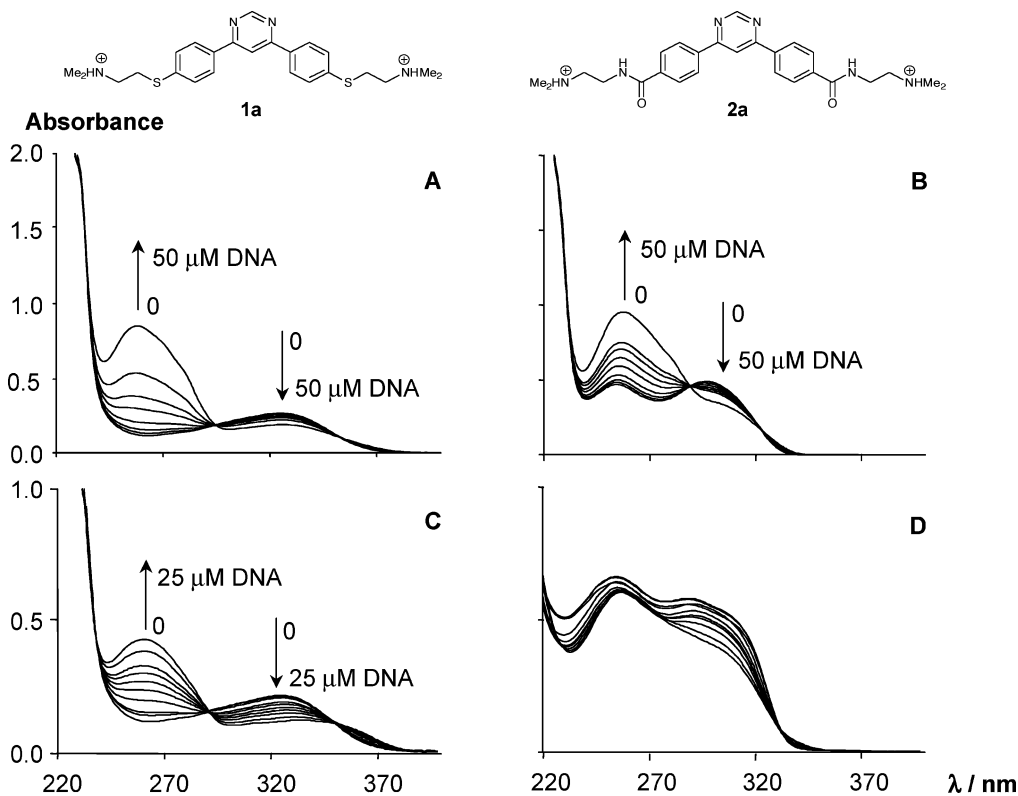


Figure 4. UV-visible absorbance spectra for the titration addition of poly(dA)·poly(dT) duplex (A, B) and poly(dA)·[poly(dT)]₂ triplex (C, D) into ligand solutions (fixed at 25 μM) containing either thioether **1a** (A, C) or amide **2a** (B, D). Spectral changes are indicated for equilibrated DNA–drug mixtures containing 0, 1, 2, 5, 10, 15, 20, 25, and 50 μM (bp) duplex or 0, 1, 2, 5, 7.5, 10, 12.5, 15, 20, and 25 μM (bt) triplex.

thioether **1a** (Figure 4C) or amide **2a** (Figure 4D), where the thioether again produced sharp isosbestic points and hypochromicity indicative of interaction between the ligand and DNA triplex in a discrete binding mode. In contrast, no such interactions were apparent for amide **2a** with this triplex, again mirroring the effects seen in denaturation experiments with CT DNA. The structural basis for these differential behaviors and for the selective destabilization of triplex DNA is uncertain and the subject of continuing investigations.

Competition Equilibrium Dialysis: Nucleic Acid Structure Binding Preferences. This competitive assay is an important tool in discerning ligand–nucleic acid interactions and binding preferences for nucleic acid structures.^{45–48} Briefly, a common pool of test ligand is dialyzed against an array of competing nucleic acid structures in a single experiment. At equilibrium, the free ligand concentration will be the same for each dialysis compartment and the amount bound to each structure indicates the binding affinity. Thus, binding constants and energies can be obtained in a direct and quantitative manner. Data obtained for a range of biarylpyrimidines from the thioether (**1**) and amide (**2**) series dialyzed against a panel of 18 nucleic acid structures are presented in Figure 5; derived thermodynamic parameters are collected in Table 2.⁴⁹

These results broadly confirm that neither ligand class shows a strong affinity for any nucleic acid duplex or single-stranded structure examined in the assay, irrespective of either sequence or backbone involved. As anticipated, preferential interactions were instead evident for high-order nucleic acid structures. The simple thioethers **1a,b** showed a strong preference for triplex DNA (27-fold greater than for the natural duplex, calf thymus (CT) DNA). Significantly, less ligand is bound to triplex RNA, indicating that at least part of the bound ligand (probably the pendent side chains) must align in the grooves of the DNA triplex, an accommodation thwarted by the 2'-hydroxyl groups

in the all-RNA structure.^{21,22} In contrast, the amides **2** bind preferentially to quadruplex DNA structures but are less discriminating in their overall recognition profiles. Neutral compounds ($Z = \text{OH}$ or OMe) showed reduced affinity for nucleic acids, but the structure preferences generally resemble those of their dimethylamino counterparts. In both series, variation of the simple dialkylamino groups only influenced binding affinity (e.g., $Z = \text{NMe}_2 > \text{NEt}_2$) while the overall selectivity was unaffected. However, compounds bearing saturated heterocyclic side chains show different patterns of binding preferences that are also reflected in their anomalous thermal melting behavior.

Results from selected quantitative analysis of the competition equilibrium dialysis data using established methods⁵⁰ are presented in Table 2. Apparent binding constants (K_{app}) and free energies of binding (ΔG) are presented for thioethers with their preferred host poly(dA)·[poly(dT)]₂ triplex nucleic acid structure and for amides with the [d(T₂G₂₀T₂)]₄ parallel-stranded DNA quadruplex. Data for the natural CT DNA duplex are included for comparison. Parameter errors have previously been estimated as 10–15%.⁴² Two further analytical descriptors can be used to quantitate binding selectivity: (i) the specificity sum (SS) given by summation of the normalized amounts bound to each DNA structure and (ii) the ratio C_{max}/SS . In the present assay system, SS would have a value between 1 (i.e., perfect selectivity for a single structure) and 18, where the latter value requires that equal amounts are bound to all of the 18 competing structures (i.e., a complete absence of selectivity). The C_{max}/SS parameter provides a simple indicator for both binding affinity and inherent selectivity, where C_{max} is the largest amount of ligand bound to any structure in the assayed nucleic acid panel. From the experimental results of competition equilibrium dialysis with 126 compounds from a diverse range of chemical classes and an alternative array of 13 nucleic acid structures,

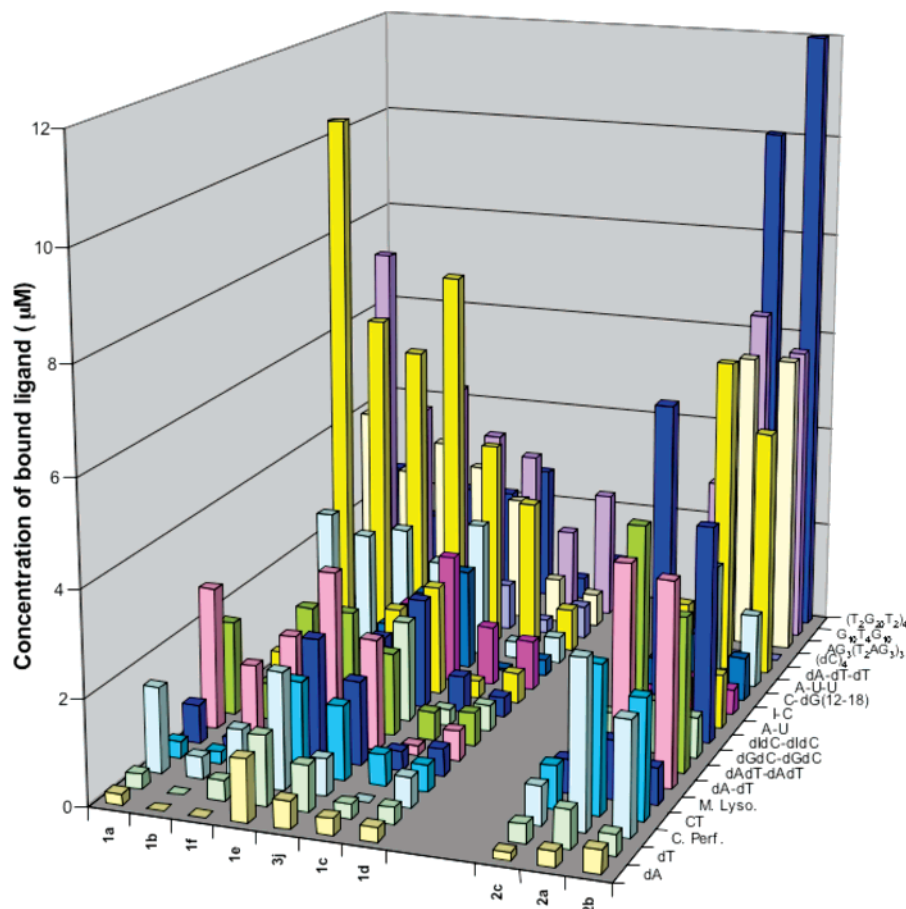


Figure 5. Competition equilibrium dialysis data for compounds **1a–f** (left) and **2a–c** (right). The vertical columns indicate the relative binding of each candidate ligand to the nucleic acid system. For a description of the nucleic acid structures used, see Table S1 (Supporting Information).

Table 2. Thermodynamic Parameters Derived from Competition Equilibrium Dialysis Data for Test Ligands against a Panel of 18 Nucleic Acid Structures

ligand	C_b μM	triplex ^a $K_{\text{app}}, 10^5 \text{ M}^{-1}$	duplex ^b $K_{\text{app}}, 10^5 \text{ M}^{-1}$	$\Delta G_{\text{triplex}}$ kcal mol^{-1}	ΔG_{CTDNA} kcal mol^{-1}	SS	C_{max}/SS	$\Delta\Delta G_{\text{triplex,CT}}$ kcal mol^{-1}	$\Delta\Delta G_{\text{triplex,1a}}$ kcal mol^{-1}
1a	10.4	1.60	0.04	−5.66	−3.54	3.35	3.09	−2.12	0.00
1b	6.4	0.93	0.03	−5.34	−3.32	3.21	1.99	−2.02	0.32
1c	2.9	0.41	0.08	−4.86	−3.91	3.85	0.76	−0.95	0.80
1d	0.8	0.11	0.07	−4.10	−3.82	4.88	0.51	−0.29	1.55
1e	7.4	1.09	0.24	−5.43	−4.55	5.46	1.35	−0.89	0.22
1f	5.8	0.84	0.06	−5.28	−3.77	4.80	1.21	−1.51	0.38
3j	4.0	0.57	0.19	−5.05	−4.42	8.73	0.46	−0.64	0.61
ligand	C_b μM	quadruplex ^c $K_{\text{app}}, 10^5 \text{ M}^{-1}$	duplex $K_{\text{app}}, 10^5 \text{ M}^{-1}$	$\Delta G_{\text{quadruplex}}$ kcal mol^{-1}	ΔG_{CTDNA} kcal mol^{-1}	SS	C_{max}/SS	$\Delta\Delta G_{\text{quadruplex,CT}}$ kcal mol^{-1}	$\Delta\Delta G_{\text{quadruplex,2a}}$ kcal mol^{-1}
2a	10.0	1.55	0.39	−5.64	−4.83	5.81	1.73	−0.8	0.00
2b	12.5	2.00	0.31	−5.79	−4.70	4.05	3.09	−1.1	−0.15
2c	3.0	0.42	0.11	−4.87	−4.10	5.12	0.59	−0.8	0.76

^a Poly(dA)·[poly(dT)]₂. ^b CT DNA. ^c [d(T₂G₂₀T₂)₄].

C_{max}/SS was found⁴² to range from 0.06 to 9.8 with a mean value of 2.4 ± 2.2 .

The highest-affinity triplex-binding ligand (thioether **1a**) has $K_{\text{app}} = 1.60 \times 10^5 \text{ M}^{-1}$ for the triplex compared with $K_{\text{app}} = 0.04 \times 10^5 \text{ M}^{-1}$ for the CT DNA duplex. This $K_{\text{app}}(\text{triplex})/K_{\text{app}}(\text{CT DNA}) = 40$ ratio corresponds to $\Delta\Delta G \approx -2 \text{ kcal mol}^{-1}$ between the two systems. This energy difference indicates a significant discrimination between the host DNA structures shown by this ligand. However, the overall specificity for ligand **1a** (SS = 3.35) is less impressive, indicating that other structures, principally those rich in dA·dT base pairs, are also favored for binding. The diethyl congener **1b** was marginally more selective in its interactions (SS = 3.21). The difference

between the two ligands is more pronounced when the data are compared for binding affinity and specificity, with $C_{\text{max}}/\text{SS} = 3.09$ and 1.99 for **1a** and **1b**, respectively. The marked difference in behavior for the diethylamine **1b** and piperidinyl **1c** (SS = 4.80, $C_{\text{max}}/\text{SS} = 1.21$) derivatives highlights the effect of side chain flexibility on binding such that the more rigid piperidinyl compound has both reduced affinity and discrimination in its binding interactions.

In contrast to the thioethers, the preferred nucleic acid targets for the amide ligands are the three quadruplex DNA forms: the folded human telomeric intramolecular $d[\text{AG}_3(\text{T}_2\text{AG}_3)_3]$ quadruplex, the intermolecular G-wire $[d(\text{G}_{10}\text{T}_4\text{G}_{10})_n]$ structure, and the parallel-stranded $[d(\text{T}_2\text{G}_{20}\text{T}_2)_4]$ arrangement. While

Table 3. Chemosensitivity Data from the NCI Three-Cell-Line Prescreen

Compound	Z	Cell growth, % control		
		MCF-7	NCI-H460	SF-268
100 μ M				
1b	NEt ₂	83	98	85
1c	OH	97	99	119
1d	OCH ₃	33	94	106
1e		95	96	102
1f		68	98	79
2a	NMe ₂	96	100	108
2c	OH	83	104	104

qualitatively similar binding to the three quadruplexes was evident, in certain cases (**2a,b**), a modest selectivity (≤ 2 -fold) is seen for the discrete four-stranded [d(T₂G₂₀T₂)]₄ structure used for comparative analysis in Table 2. For compounds **2a** and **2b**, $K_{app} = 1-2 \times 10^5 \text{ M}^{-1}$ are seen. However, binding discrimination toward this structure rather than a standard “random” sequence duplex (CT DNA) is an order of magnitude lower, with the $K_{app(\text{quadruplex})}/K_{app(\text{CT DNA})} \approx 4.0$ ratio representing a differential $\Delta\Delta G \approx -1 \text{ kcal mol}^{-1}$. Overall, the diethylamino-terminated ligand **2b** gave the best combination of affinity and selectivity in the amide series, with $C_{max}/SS = 3.09$. Significantly, for both series, the poorest values of $C_{max}/SS < 1$ are characteristic of compounds with uncharged side chains.

The primary SAR determinant discerned from these data is that the fundamental binding preference for high-order DNA structures is largely directed by the biarylpyrimidine core structure. The chalcogen-linked compounds, thioether or ether (data not shown), favor triplex binding, while the amide linkage switches this preference to quadruplex. Within each class, the cationic side chains make a significant contribution to binding affinity while having little effect on the overall patterns of discrimination observed across the panel of 18 target structures.

The $\Delta\Delta H_{vH}$ enthalpies calculated for the DNA–ligand complexes relative to the free DNA show clear differences in thermal stabilization of nucleic acid targets between the thioether **1** and amide **2** series (determined by partial qualitative van't Hoff analysis of the UV thermal melting curves; see Supporting Information) and support the switch in binding preference. Thus, the rank order for triplex T_m^1 stabilization is given by **1a** \gg **2a**, whereas the order is reversed for duplex T_m^2 stabilization (i.e., **2a** $>$ **1a**). This behavior is reflected in the ΔT_m values (Table 1). The **1a** $>$ **2a** ranking for stabilization of duplex form of CT DNA again reflects the T_m stabilization afforded by the ligands, although the altered AT/GC binding preference here prevents a full analysis with this “pseudorandom” host DNA duplex system.

Chemosensitivity and Telomerase Inhibition. Selected compounds were assessed for in vitro chemosensitivity in the NCI three-cell-line prescreen (Table 3). In agreement with the low binding affinities determined for duplex DNA ($K_{app} \leq 4 \times 10^4 \text{ M}^{-1}$), no compound examined showed appreciable cytotoxicity toward a range of human tumor cell lines ($IC_{50} \geq 100 \mu\text{M}$). Ligands selective for quadruplex rather than duplex DNA structures have been identified as inhibitors of telomerase.^{2,17,51,52} Telomerase inhibition was assessed using the commercially

available TRAP assay⁵³ (see Supporting Information). As expected for quadruplex-binding ligands, moderate inhibition of human telomerase function was found, where the lowest $^{tel}IC_{50} \approx 10 \mu\text{M}$ activity compares favorably with that for porphyrin and perylene ($^{tel}IC_{50} \geq 10 \mu\text{M}$)^{54–56} inhibitors and the internal reference inhibitor used in this assay (BSU-1021, $^{tel}IC_{50} = 4.9 \mu\text{M}$)^{57,58} (see Supporting Information). The **2b** $>$ **2a** \sim **1f** $>$ **1a** $>$ **1d** ranking of inhibitory activities determined for the functionalized biarylpyrimidine compounds broadly reflects their relative DNA-binding strengths with the human telomeric quadruplex DNA structure d(AG₃[T₂AG₃]₃). Stabilization of the folded quadruplex (or G-quadruplex) structure is proposed to prevent access of the telomerase enzyme to the unfolded DNA substrate required for processivity in telomeric 3' extension.

Conclusion

Functionalized 4,6-biarylpyrimidines present a versatile and intriguing platform for the development of ligands for the recognition of high-order (triplex and quadruplex) nucleic acid structures. A new, flexible, and high-yielding synthesis of these agents has been developed that incorporates a Suzuki cross-coupling reaction to generate the biarylpyrimidine core structure. Two distinct classes of candidate ligand were synthesized where the side chains are linked to the aryl core structure via thioether (**1**) or amide (**2**) functional groups.

Spectrophotometric and competition equilibrium dialysis assays have revealed interesting patterns of nucleic acid binding behavior in terms of structural selectivity for the host system. Further, relatively minor alterations in ligand structure effect a dramatic switch in binding preference. Significantly, all members of both classes of ligand were indifferent binders toward duplex nucleic acid structures; binding constants $K_{app} < 4 \times 10^4 \text{ M}^{-1}$ with the mammalian CT DNA reference were obtained by the competition equilibrium dialysis method. The cationic pendent side chains are critically important to both classes of ligand in conferring a strong binding affinity. Thus, even substituent groups with a combination of H-bond donors and acceptors were unable to compensate for the absence of a formal positive charge.

UV spectrophotometry gave the first indications of discrimination in the interactions of the test ligands between duplex and triplex structures. Cationic thioethers showed appreciable thermal stabilization of the poly(dA)·[poly(dT)]₂ triplex ($\Delta T_m \leq 20 \text{ }^\circ\text{C}$) while having a negligible effect on the poly(dA)·poly(dT) duplex. The converse behavior was evident for the cationic amides where binding-induced stabilization was greater for duplex-form DNA rather than for triplex-form DNA. This structural preference was confirmed by the absence of isosbestic points and hypochromicity in titration experiments involving poly(dA)·[poly(dT)]₂ triplex and the cationic amide **2a** ligand.

A detailed picture of the nucleic acid binding properties was obtained by the competition equilibrium dialysis method. This assay reveals that neither class of ligand binds in a preferential manner to any single- or double-stranded DNA structure. Instead, in both cases, preferred binding is shown toward multistranded triplex or quadruplex structures. The overall structural preference is dictated by the functional group linking the side chain, with a switch between three-stranded (thioether, **1**) and four-stranded (amide **2**) hosts. Within each class, the overall pattern of binding preferences is similar, with uncharged substituent moieties showing reduced binding affinity and less selectivity (i.e., smaller C_{max}/SS).

The more rigid saturated heterocyclic side chains (**1e,f** and **2e–g**) have distinct effects upon the overall recognition properties for the ligands compared with acyclic groups of similar size (**1b, 2b**). Thus, in the thioether series, a marked increase in SS is accompanied by a lower binding affinity. For the amides (**2e–g**) a specific and unexpected destabilization of the triplex structure was discovered.

The molecular basis for a switch in structural binding preference following alteration in the side chain linkage is not fully understood. Molecular modeling exercises support the design rationale that superior π -stacking and drug fits for stacked G-tetrads (quadruplex) are obtained with the extended amide linkage rather than the inherently more flexible thioether. Pendent cationic charges promote this structural preference. In contrast, for triplex binding by the thioethers, the equilibrium dialysis data indicate a groove binding contribution to the interaction. Again, modeling studies support the hypothesis, but diagnostic biophysical evidence has proved elusive; stepwise NMR titration of ligand **1a** with poly(dA)·[poly(dT)]₂ triplex (in either direction) resulted in apparently quantitative precipitation of the complex rather than observable chemical shift perturbations. Detailed investigation of the key nucleic acid binding interactions and the molecular basis for the observed effects is a continuing effort, focusing upon structural studies and calorimetric and thermodynamic analyses with optimized ligand molecules to dissect the component energetic terms for the thioether and amide classes.

A subset of compounds was assayed as inhibitors of human telomerase and a moderate ^{tel}IC₅₀ ≈ 10 μM was found, consistent with modest, unoptimized binding ($K_{app} = 0.85 \times 10^5 \text{ M}^{-1}$) to the human telomeric sequence AG₃(T₂AG₃)₃. Significantly, both weak duplex DNA binding and concomitant low cytotoxicity (IC₅₀ > 100 μM) were determined. These findings will be important for future development of such agents as selective modulators of gene expression through interaction with high-order DNA structures. In summary, the 4,6-biarylpyrimidine ligands are an attractive class of compounds for diversification and optimization of their nucleic acid recognition properties. These agents are synthetically accessible, nontoxic, and not complicated by the photosensitivity problems that hamper other ligands with extended aromatic chromophores (e.g., porphyrins, quinones, coralyne) reported for use in targeting high-order nucleic acid systems.

Experimental Section

UV Thermal Melting Studies. Calf thymus (CT) DNA and poly[dA]·poly[dT] and poly[dT] DNA were purchased from Sigma as the sodium salts and used without further purification. An aqueous buffer containing 10 mM Na₂HPO₄/NaH₂PO₄, 1 mM Na₂EDTA, pH 7.00 ± 0.01, was used for CT DNA melting experiments. An aqueous buffer containing 10 mM sodium cacodylate, 300 mM NaCl, 0.1 mM Na₂EDTA, pH 6.00 ± 0.01, was used for triplex DNA melting experiments. Concentrations of all DNA solutions were determined by UV spectrophotometry using the following extinction coefficients: CT DNA, $\epsilon_{260} = 12\,824 \text{ (M (base pairs))}^{-1} \text{ cm}^{-1}$; poly[dA]·poly[dT], $\epsilon_{260} = 12\,000 \text{ (M (base pairs))}^{-1} \text{ cm}^{-1}$; poly[dT], $\epsilon_{265} = 8700 \text{ (M (nucleotides))}^{-1} \text{ cm}^{-1}$. The poly[dA]·poly[dT]₂ triplex was formed by mixing equimolar (i.e., base pairs to nucleotides) solutions of the poly[dA]·poly[dT] duplex and the poly[dT] single strand, then annealing by heating to 95 °C followed by slow cooling overnight.

Ligands were dissolved in buffer or DMSO, ensuring that the ultimate concentration of DMSO was ≤1–2% v/v where used. DMSO calibration curves were used to correct the T_m values. Ligand stock solutions were stored in the refrigerator (0–5 °C) when not in use.

UV DNA melting curves were determined using a Varian-Cary 400 Bio UV/vis spectrophotometer equipped with a Peltier temperature controller. Heating runs were typically performed between 40 and 95 °C, heating at a rate of 1 °C min⁻¹, while the absorbance at 260 nm was continuously monitored. All melts were performed in 1 cm path length quartz cells. Solutions of DNA and the candidate ligand were prepared by direct mixing of a solution containing either CT DNA or triplex with aliquots from the ligand stock solution. Melting temperatures were determined from the primary data using the method of Wilson et al.⁴⁴

Spectrophotometric Titrations. The experimental procedure used for equilibrium binding titration experiments has been published.⁵⁹ Concentrated stock solutions of ligands **1a** and **2a** (~3 mM) were freshly prepared in DMSO and diluted to the required concentration with either aqueous phosphate or cacodylate buffer (see above), as required. Stock aqueous solutions containing either poly(dA)·poly(dT) or poly(dA)·[poly(dT)]₂ at known high concentration (~5 mM in bp or bt for the duplex and triplex, respectively) were similarly prepared in the appropriate buffer system. UV-visible absorbance spectra were recorded at 25 °C for aqueous solutions containing the ligand (500 μL of 25 μM) in a quartz cuvette using a Varian-Cary 400BIO instrument. Serial aliquot portions of DNA stock solution were then added to generate working solutions containing the reactants at several defined molar ratios (see Figure 4). The spectrum was rerecorded at each titer step following equilibrium stirring at 25 °C for 15 min. Spectra were similarly recorded for mixtures containing a large known molar excess of the DNA to determine isosbestic behavior and the saturation approach to binding equilibrium.

Competition Dialysis. Competition dialysis experiments were performed exactly as previously described,^{45,47,49} albeit with a new array of nucleic acid structures. The nucleic acids structures used in the new test array are listed in Table S2 of Supporting Information. The preparation and tests for the quality of these nucleic acids are fully described in refs 45 and 49. Competition dialysis studies were performed in BPES buffer, consisting of 6 mM Na₂HPO₄, 2 mM NaH₂PO₄, 1 mM Na₂EDTA, 185 mM NaCl, pH 7.0. Test ligand molecules (1 μM concentration, 200 mL volume) were dialyzed against the nucleic acid array. Each nucleic acid structure was at 75 μM in a volume of 200 μL. Following 24 h of dialysis, samples were removed and ligand was dissociated by the addition of SDS to a final concentration of 1% (v/v). The total ligand concentration present in each nucleic acid sample was measured spectrophotometrically using microcuvettes at an absorbance maximum appropriate for each ligand and corrected for the slight dilution resulting from the addition of the SDS solution. The free ligand concentration, which typically was not appreciably different from the initial concentration of 1 μM, was determined spectrophotometrically from an aliquot of the dialysate solution, and the concentration of ligand bound to each nucleic acid structure was determined by difference ($C_b = C_i - C_f$).

Synthesis. Boronic acids were purchased from Frontier Scientific, Europe Ltd., Carnforth, Lancashire, U.K. Other reagents were purchased from Sigma-Aldrich, Gillingham, U.K., or Lancaster, Morecambe, U.K. Solvents were purchased from Riedel-de Haën and, where stated, purified according to Perrin, Perrin, and Armarego.⁶⁰ TLC was performed on highly purified silica gel plates with UV indicator (silica gel 60 F₂₅₄), manufactured by Merck and visualized under UV light (254 or 366 nm) or stained with iodine. Flash chromatography was performed using silica gel (40–63 μm) purchased from Merck and used following the methodology described by Still et al.⁶¹ Melting points were determined using an Electrothermal IA9200 digital melting point apparatus. Infrared data were obtained on a Perkin-Elmer (Paragon 1000) FT-IR spectrophotometer. Routine nuclear magnetic resonance spectra were acquired on a JEOL GX270Delta spectrometer (observing ¹H at 270.17 MHz and ¹³C at 67.80 MHz). Alternatively, where stated, a JEOL ECA600 spectrometer (observing ¹H at 600.17 MHz and ¹³C at 150.91 MHz) was used. ¹³C assignments were made with the aid of the DEPT135 experiment. Values of J and δ of aryl AB systems were calculated using the NMRcalc program (T. C. Jenkins,

2001). Mass spectra were obtained from the EPSRC National Mass Spectrometry Service Centre, University of Wales, Swansea. Elemental analysis was performed by the Advanced Chemical and Materials Analysis Unit at the University of Newcastle upon Tyne, U.K.

General Method 1: Suzuki Coupling Reaction. 4,6-Bis(4-methoxyphenyl)pyrimidine-0.25H₂O, 3c. A solution of 4-methoxyphenylboronic acid (0.9 g, 5.9 mmol), 4,6-diiodopyrimidine, (0.98 g, 2.9 mmol), palladium(0)tetrakis(triphenylphosphine) (45.6 mg, 0.04 mmol), and K₂CO₃ (0.58 g, 5.9 mmol) in toluene/EtOH (9:1 v/v, 200 mL) was thoroughly degassed using a stream of dry N₂, then stirred vigorously under reflux. After 8 h the solution was concentrated by evaporation under vacuum and the residue partitioned between H₂O and ether (50 + 50 mL) and extracted with ether (3 × 100 mL). The combined organic extracts were dried over MgSO₄ and evaporated. Recrystallization from EtOH afforded biarylpyrimidine **3c** as a white solid (0.52 g, 61%): mp 148–149 °C; ¹H NMR (CDCl₃, 600.17 MHz) δ 9.20 (d, *J* = 1.3 Hz, 1H, 2-H), 8.11 (1/2AB, *J* = 8.9 Hz, 4H, 2'-H, 6'-H), 7.97 (d, *J* = 1.3 Hz, 1H, 5-H), 7.03 (1/2AB, *J* = 8.9 Hz, 4H, 3'-H, 5'-H), 3.89 (s, 6H, OCH₃); ¹³C NMR (CDCl₃) δ 165.1 (C-4, C-6), 163.4 (C-4'), 159.0 (C-2), 128.7 (1'), 123.1 (C-2', C-6'), 114.4 (C-3', C-5'), 111.0 (C-5), 55.4 (CH₃); IR (CH₂Cl₂) 3450w, 1600s, 1590s, 1575s, 1510s, 1405s cm⁻¹; MS (FAB) (%) 293 ([M + H]⁺, 100), 152 (17), 107 ([C₆H₄OCH₃]⁺, 36); UV-vis (10 mM sodium phosphate buffer, pH 7.00, 1 mM EDTA, 300 mM NaCl) λ_{max} (nm) [ε (M⁻¹ cm⁻¹)] 332 [6026]. Anal. (C₁₈H₁₆N₂O₂·0.25H₂O) C, H, N.

4,6-Bis(4-methoxycarbonylphenyl)pyrimidine, 3a. **3a** was prepared by general method 1 from 4-methoxycarbonylphenylboronic acid (1.74 g, 9.64 mmol). Solvents were removed by evaporation, and the product was recrystallized from ethyl acetate to yield 1.53 g (91%); mp 223.5–225.0 °C; ¹H NMR (CDCl₃, 600.17 MHz) δ 9.38 (d, *J* = 1.4 Hz, 1H, 2-H), 8.21 (AB, 8H, 2'-H, 3'-H, 5'-H, 6'-H), 8.19 (d, *J* = 1.4 Hz, 1H, 5-H), 3.97 (s, 6H, OCH₃); ¹³C NMR (DMSO) δ 166.1 (C=O), 163.2 (C-4, C-6), 159.4 (C-2), 140.6 (C-1'), 132.0 (C-4'), 129.9 (C-3', C-5' or C-2', C-6'), 127.9 (C-2', C-6' or C-3', C-5'), 114.2 (C-5), 52.9 (OCH₃); IR (CH₂Cl₂) 1725s (C=O), 1580s, 1460m, 1105m, 1020w cm⁻¹; MS (EI) (%) 348 (M⁺, 87), 317 ([M - OCH₃]⁺, 100), 289 (82), 203 (26), 101 (49). Anal. (C₁₉H₁₆N₂O₄) C, H, N.

4,6-Bis(4-bromophenyl)pyrimidine-0.25H₂O, 3b. Treatment of diiodopyrimidine (1.92 g, 6.03 mmol) with 4-bromophenylboronic acid (2.42 g, 12.05 mmol), according to general method 1, afforded biarylpyrimidine **3b** as white crystals from ethanol (1.6 g, 68%); mp 196.5–197.5 °C; ¹H NMR (CDCl₃, 600.17 MHz) δ 9.29 (d, *J* = 1.1 Hz, 1H, 2-H), 8.04 (d, *J* = 1.1 Hz, 1H, 5-H), 8.02 (1/2AB, *J* = 8.6 Hz, 4H, 2'-H, 6'-H), 7.67 (1/2AB, *J* = 8.6 Hz, 4H, 3'-H, 5'-H); ¹³C NMR (CDCl₃) δ 164.5 (C-4, C-6), 160.0 (C-2), 137.0 (C-1'), 133.0 (C-2', C-6'), 129.4 (C-3', C-5'), 126.6 (C-4'), 112.8 (C-5); IR (CH₂Cl₂) 1580s, 1520m, 1460m, 1260w, 1075w cm⁻¹; MS (CI) (%) 388 + 390 + 392 (M⁺ 54%, 1:2:1 isotopic distribution for ⁸¹Br/⁸¹Br, ⁸¹Br/⁷⁹Br, ⁷⁹Br/⁷⁹Br), 311 + 309 ([M - Br]⁺, 32), 284 + 282 (36), 229 ([M - 2Br]⁺, 22), 203 (50), 101 (100). Anal. (C₁₆H₁₀Br₂N₂·0.25H₂O) C, H, N.

4,6-Bis(4-fluorophenyl)pyrimidine, 3d. By General Method 1. 4-Fluorophenylboronic acid (3.97 g, 27.51 mmol), 4,6-dichloropyrimidine (2.06 g, 13.42 mmol), and finely powdered K₂CO₃ (5.56 g) in methanol/toluene (1:9, 300 mL) were mixed with strong agitation and thorough degassing with N₂ for 30 min at 60 °C. Pd(Ph₃P)₄ (0.3 g) was added, and the mixture was heated to reflux with strong agitation for 6 h. The solvent was evaporated and the residue partitioned between chloroform (3 × 150 mL) and water (200 mL). The organic layers were combined, dried over MgSO₄, filtered, and evaporated to dryness. The residue was recrystallized from methanol and water (2.93 g, 82%): mp 102.6–103.6 °C (lit.²⁴ 88.9–90.6 °C). All NMR data obtained are consistent with the assigned structure but different from those quoted in the literature.²⁴ ¹⁹F NMR (CDCl₃, 564.73 MHz, CFCl₃ reference) δ -109.2; ¹H NMR (CDCl₃, 600.17 MHz) δ 9.25 (d, *J* = 1.2 Hz, 1H, 2-H), 8.13 (dd, ³J_{HH} = 8.7, ⁴J_{HF} = 5.3 Hz, 4H, 2'-H, 6'-H), 7.98 (d, *J* = 1.2 Hz, 1H, 5-H), 7.21 (t, ³J_{HH} ≈ ³J_{HF} = 8.7 Hz, 4H, 3'-H, 5'-H);

¹³C{¹H} NMR (CDCl₃, 150.91 MHz) δ 164.8 (d, ¹J_{CF} = 252.9 Hz, C-4'), 163.7 (C-4, C-6), 159.3 (C-2), 133.1 (d, ⁴J_{CF} = 4.3 Hz, C-1'), 129.3 (d, ³J_{CF} = 10.1 Hz, C-2', C-6'), 116.2 (d, ²J_{CF} = 21.7 Hz, C-3', C-5'), 112.1 (C5); IR (CH₂Cl₂) 1600s, 1573s, 1510s, 1450s, 1275s, 850s cm⁻¹. MS (ES⁺) (%) 269 (100) (M + H)⁺, Anal. (C₁₆H₁₀F₂N₂) C, H, N.

4,6-Bis(4-tert-butylmercaptophenyl)pyrimidine, 3e. A slurry of 4,6-bis-(4-fluorophenyl)pyrimidine **3d** (1.26 g, 4.70 mmol) and sodium *tert*-butylthiolate (1.16 g, 10.34 mmol) in DMF (25 mL) was heated at 70 °C for 18 h. Water (50 mL) was added to the reaction mixture, and the solution was extracted with ether (1 × 150 mL, 2 × 50 mL). The combined organic extracts were dried over MgSO₄, filtered, and evaporated. Recrystallization from ethanol gave fine, colorless needles (1.60 g, 84%): mp 151.5–152.5 °C; ¹H NMR (CDCl₃, 600.17 MHz) δ 9.29 (d, *J* = 1.2 Hz, 1H, 2-H), 8.09 (d, *J* = 1.2 Hz, 1H, 5-H), 8.08 (1/2AB, *J* = 8.4 Hz, 4H, 2'-H, 6'-H), 7.66 (1/2AB, *J* = 8.4 Hz, 4H, 3'-H, 5'-H), 1.31 (s, 18H, C(CH₃)₃); ¹³C NMR (CDCl₃, 150.91 MHz) δ 163.9 (C-4, C-6), 159.3 (C-2), 137.8 (C-2', C-6'), 137.2 and 136.6 (C-1' and C-4'), 127.2 (C-3', C-5'), 112.9 (C5), 46.6 (CMe₃), 31.2 (CH₃); IR (CH₂Cl₂) 2950m, 1575s, 1505s, 1450s, 1270s cm⁻¹; MS (ES⁺) (%) 409 (100) (M + H)⁺. Anal. (C₂₄H₂₈N₂S₂) C, H, N.

4,6-Bis(4-trichloromethylsulfanylphenyl)pyrimidine, 3f. A solution of 4,6-bis(4-*tert*-butylmercaptophenyl)pyrimidine **3e** (0.078 g, 0.2 mmol) and CCl₃SCl (0.402 g, 2.2 mmol) in acetic acid (8 mL) was heated at 50 °C for 24 h. The mixture was partitioned between ethyl acetate (100 mL) and water (100 mL). The organic layer was separated, dried over MgSO₄, filtered, and evaporated. The pale-yellow solid was recrystallized from ethanol (0.088 g, 78%): mp 126.1–127.3 °C; ¹H NMR (270.17 MHz, CDCl₃) δ 9.31 (d, *J* = 1.0 Hz, 1H, 2-H), 8.14 (1/2AB, *J* = 8.5 Hz, 4H, 2'-H, 6'-H), 8.07 (d, *J* = 1.0 Hz, 1H, 5-H), 7.80 (1/2AB, *J* = 8.5 Hz, 4H, 3'-H, 5'-H), 3.70 and 1.23 (q and t, EtOH); ¹³C NMR δ 163.8 (C-4, C-6), 159.2 (C-2), 138.7 and 136.6 (C-1' and C-4'), 129.2 (C-3', C-5' or C-2', C-6'), 128.1 (C-2', C-6' or C-3', C-5'), 112.7 (C-5), SCCL₃ not observed; IR (CH₂Cl₂) 1575s, 1510s, 1450m, 1290m, 1010w, 825s cm⁻¹; MS (ES⁺) (%) 474 (100) (M + H)⁺. Anal. (C₁₈H₁₀Cl₆N₂S₄·0.25EtOH) C, H, N.

4,6-Bis[4-(2-nitrophenylsulfanyl)phenyl]pyrimidine, 3g. A solution of 4,6-bis(4-*tert*-butylmercaptophenyl)pyrimidine **3e** (3.680 g, 9.0 mmol) and 2-nitrobenzenesulfenyl chloride (6.83 g, 36.0 mmol) in acetic acid (130 mL) was heated at 65 °C for 2 h. The mixture was cooled to -20 °C, filtered, and washed with ethanol. The yellow solid was triturated with hot ethanol and filtered hot (4.35 g, 86%): mp 220–222 °C; ¹H NMR (270.17 MHz, CDCl₃) δ 9.26 (d, *J* = 1.0 Hz, 1H, 2-H), 8.58 (d, *J* = 1.0 Hz, 1H, 5-H), 8.37 (d, *J* = 8.5 Hz, 2H, 3''-H), 8.34 (1/2AB, *J* = 8.5 Hz, 4H, 2'-H, 6'-H), 8.08 (d, *J* = 8.5 Hz, 2H, 6''-H), 7.86 (t, *J* = 8.5 Hz, 2H, 4''-H), 7.72 (1/2AB, *J* = 8.5 Hz, 4H, 3'-H, 5'-H), 7.57 (t, *J* = 8.5 Hz, 2H, 5''-H); ¹³C NMR (CDCl₃, 150.91 MHz) δ 163.4 (C-4, C-6), 159.5 (C-2), 145.8 (C-2''), 138.4 (C-1'), 136.1 (C-4'), 136.0 (C-3'), 135.1 (C-4'), 128.9 (C-2', C-6'), 127.9 (C-3', C-5'), 128.3, 127.4 and 127.1 (C-4'', C-5'', and C-6''), 112.9 (C-5); IR (KBr) 1585s, 1510s, 1335s, 1300m, 725m cm⁻¹; MS (ES⁺) (%) 603 (50) (M + H)⁺. Anal. (C₂₈H₁₈N₄O₄S₄·H₂O) C, H, N.

4,6-Bis(4-carboxyphenyl)pyrimidine-0.5H₂O, 3h. 4,6-Bis[4-methoxycarbonylphenyl]pyrimidine **3a** (0.67 g, 1.92 mmol) was added to 2 M NaOH solution (50 mL) and heated under reflux for 12 h. The solution was left to cool and was then acidified (pH 6) using concentrated HCl. The resultant precipitate was collected by filtration, washed with water, ethanol, and ether, and then dried to yield 0.61 g of a white solid (100%): mp > 300 °C (dec); ¹H NMR (DMSO) δ 13.06 (br s, 1H, OH), 9.39 (s, 1H, 2-H), 8.79 (s, 1H, 5-H), 8.51 (1/2AB, *J* = 8.4 Hz, 4H, 2'-H, 6'-H), 8.12 (1/2AB, *J* = 8.4 Hz, 4H, 3'-H, 5'-H); ¹³C NMR (DMSO) δ 167.3 (C=O), 163.4 (C-4, C-6), 159.3 (C-2), 139.9 (C-1'), 134.1 (C-4'), 130.0 (C-3', C-5'), 127.6 (C-2', C-6'), 113.9 (C-5); IR (KBr) 3020w (OH), 1690m (CO₂H) 1100s cm⁻¹; MS (ES) (%) 321 (M + H, 100). Anal. (C₈H₁₂N₂O₄·0.5H₂O) C, H, N.

4,6-Bis(4-ethylmercaptophenyl)pyrimidine, 3i. A slurry of 4,6-bis(4-bromophenyl)pyrimidine **3b** (4.84 g, 11.5 mmol) and NaSEt

(2.42 g, 28.75 mmol) in DMF (100 mL) was heated under nitrogen at 100 °C for 48 h. The residue obtained on evaporation of DMF was boiled with water (75 mL), and the solids were collected by filtration. Recrystallization from ethanol gave two crops of pale-yellow, fluffy needles (2.51 g, 62%): mp 109.2–111.2 °C; ¹H NMR (CDCl₃, 600.17 MHz) δ 9.25 (d, *J* = 1.2 Hz, 1H, 2-H), 8.06 (¹/₂AB, *J* = 8.6 Hz, 4H, 2'-H, 6'-H), 8.02 (d, *J* = 1.2 Hz, 1H, 5-H), 7.41 (¹/₂AB, *J* = 8.6 Hz, 3'-H, 5'-H), 1.38 (t, *J* = 7.4 Hz, 6H, CH₃), 3.04 (q, *J* = 7.4 Hz, 4H, SCH₂); ¹³C NMR (CDCl₃, 150.91 MHz) δ 164.0 (C-4, C-6), 159.3 (C-2), 141.4 (C-1'), 133.8 (C-4'), 127.8 (C-3', C-5' or C-2', C-6'), 127.5 (C-2', C-6' or C-3', C-5'), 111.7 (C-5), 26.7 (SCH₂), 14.2 (CH₃); IR (CH₂Cl₂) 1600m, 1575s, 1505m, 1450m, 1350w, 1100s, 850m cm⁻¹; MS (ES+) (%) 353 (100) (M + H)⁺, 324. 43. Anal. (C₂₀H₂₀N₂S₂) C, H, N.

4,6-Bis(4-mercaptophenyl)pyrimidine, 3j. NaBH₄ (2.0 g, 53.1 mmol) was dissolved in a mixture of ethanol (100 mL) and water (15 mL), pH 8–9. Disulfide **3g** (3.2 g, 5.31 mmol) was then added over 30 min. The mixture was stirred at room temperature for 2 h. Solids were removed by filtration through an elite pad, and the filtrate volume was reduced to a third. The red solution was partitioned between chloroform (4 × 250 mL) and water (200 mL), the pH being adjusted slowly with 4 M HCl to pH 4. The organic layers were combined, dried over MgSO₄, filtered, and reduced to dryness. The resulting residue was triturated with hot hexane and filtered hot to leave a yellow solid (1.25 g, 79%): mp 183–185 °C; ¹H NMR (CDCl₃) δ 9.24 (s, 1H, 2-H), 8.01 (s, 1H, 5-H), 7.98 (¹/₂AB, *J* = 8.6 Hz, 4H, 2'-H, 6'-H), 7.39 (¹/₂AB, *J* = 8.6 Hz, 4H, 3'-H, 5'-H), 3.60 (s, 2H, SH); ¹³C NMR (CDCl₃) δ 164.5 (C-4, C-6), 159.8 (C-2), 136.2 and 134.7 (C-4' and C-1'), 129.8 (C-2', C-6' or C-3', C-5'), 128.4 (C-3', C-5' or C-2', C-6'), 112.3 (C5); IR (KBr) 3400m, 1620s, 1580s, 1500m, 1375m, 1100s cm⁻¹; HRMS (CI) 297.0512 ([M + H]⁺), C₁₆H₁₃N₂O₂ requires 297.0515; MS (EI) (%) 296 (M⁺, 70), 263 ([M - S]⁺ (23), 236 (14), 134 (29), 105 (48), 44 (50), 49 (47), 43 (100).

General Method 2: Preparation of Thioethers. 4,6-Bis[4'-(2'-dimethylamino)ethyl]mercapto]phenyl]pyrimidine·2/3HBr·0.25H₂O, 1a. A mixture of bisthiophenol **3j** (0.25 g, 0.85 mmol), 2-dimethylaminoethyl chloride hydrochloride (0.37 g, 2.55 mmol), and K₂CO₃ (0.29 g, 2.12 mmol) was stirred in dry DMF (5 mL) at room temperature for 18 h. The reaction mixture was partitioned between water and ether (25 + 25 mL), and the organic layer was washed twice with water, dried over MgSO₄, filtered, and evaporated to dryness. The crude residue was suspended in dilute HBr (20 mL, 15% w/v) and stirred for 30 min. The solution was evaporated to dryness, and the crude solid was recrystallized from ethanol. Free base: ¹H NMR (CDCl₃) δ 9.21 (d, *J* = 1.1 Hz, 1H, H-2), 8.03 (¹/₂AB, *J* = 8.4 Hz, 4H, 2'-H, 6'-H), 7.97 (d, *J* = 1.1 Hz, 1H, 5-H), 7.39 (¹/₂AB, *J* = 8.4 Hz, 4H, 3'-H, 5'-H), 3.10 (t, *J* = 7.0 Hz, 4H, SCH₂), 2.59 (t, *J* = 7.0 Hz, 4H, CH₂N), 2.27 (s, 12H, NCH₃); ¹³C NMR (CDCl₃) δ 164.6 (C-4, C-6), 159.9 (C-2), 141.7 (C-4'), 134.6 (C-1'), 128.5 (C-2', C-6' or C-3', C-5'), 128.2 (C-3', C-5' or C-2', C-6'), 12.4 (C-5), 58.9 (SCH₂), 46.0 (NCH₃), 30.3 (NCH₂); IR (CH₂Cl₂) 3684w, 2948m, 1582s, 1511m, 1497m, 1460s, 1372m cm⁻¹; MS (CI) (%) 439 ([M + H]⁺, 100), 396 ([M - NMe₂]⁺, 8), 368 (54), 336 ([M - SCH₂CH₂NMe₂]⁺, 72). Hydrobromide salt: mp 258–259 °C; UV–vis (10 mM aqueous phosphate buffer, pH 7.00, 1 mM EDTA and 300 mM NaCl) λ_{max} (nm) [ε (M⁻¹ cm⁻¹)] 236 [10 636], 329 [7076]. Anal. (C₂₄H₃₀N₄S₂·2/3HBr·0.25H₂O) C, H, N.

4,6-Bis(4-[(2-(dimethylamino)ethyl)carboxamido]phenyl)pyrimidine·3HBr·1.25H₂O, 2a. A solution of ester **3a** (0.45 g, 1.28 mmol) in *N,N*-dimethylethylenediamine (20 mL) was heated under reflux for 8 h. Excess *N,N*-dimethylethylenediamine was removed by evaporation in vacuo, and the residue was purified by flash column chromatography (hexane/dichloromethane/triethylamine, 45:45:10) to give diamide **2a** (0.52 g, 88%) as a brown oil. Treatment with 48% HBr (1 mL), evaporation to dryness, and recrystallization from methanol–2-propanol gave the hydrobromide salt as a white solid: mp 219–220 °C; ¹H NMR (CDCl₃) δ 9.29 (d, *J* = 1.3 Hz, 1H, 2-H), 8.16 (¹/₂AB, *J* = 8.7 Hz, 4H, 2'-H, 6'-H), 8.09 (d, *J* = 1.3 Hz, 5-H), 7.91 (¹/₂AB, *J* = 8.7 Hz, 4H, 3'-H,

5'-H), 6.95 (br t, exch. D₂O, 2H, CONH), 3.51 (q, *J* = 5.8 Hz, 4H, CONHCH₂), 2.53 (t, *J* = 5.8 Hz, 4H, CH₂NMe₂), 2.26 (s, 12H, CH₃); ¹³C NMR 167.3 (C=O), 164.6 (C-4, C-6), 160.2 (C-2), 140.1 (C-4'), 137.5 (C-1'), 128.4 (C-2', C-6' or C3', C-5'), 128.0 (C3', C-5' or C-2', C-6'), 113.9 (C-5), 58.3 (CH₂NMe₂), 45.8 (CH₃), 37.9 (CH₂NHCO); HRMS (CI) 461.2665 ([M + H]⁺), C₂₆H₃₃N₆O₂ requires 461.2660; MS (CI) 462 ([M + 2H]⁺, 32), 461 ([M + H]⁺, 100), 447 ([M - CH₃]⁺, 6), 416 (9), 390 [M - CH₂CH₂NMe₂]⁺, 3), 193(8), 60 (50); IR (CH₂Cl₂) 3683w, 3410w, 3054m, 2951m, 1660s, 1586s, 1524s, 1497s, 1462s, 1290m cm⁻¹. Hydrobromide salt: mp 219–220 °C, UV–vis (10 mM sodium phosphate buffer, pH 7.00, 1 mM EDTA, 300 mM NaCl) λ_{max} (nm) [ε (M⁻¹ cm⁻¹)] 255 [21 670], 289 [18 338]. Anal. (C₂₆H₃₃N₆O₂·3HBr·1.25H₂O) C, H, N.

General Method 3: Preparation of Amides. 4,6-Bis(4-[(2-(diethylamino)ethyl)carboxamido]phenyl)pyrimidine·2HBr·2H₂O, 2b. 4,6-Bis(4-carboxyphenyl)pyrimidine (0.30 g, 0.94 mmol), PyBOP (1.22 g, 2.34 mmol), and triethylamine (0.33 mL, 2.34 mmol) were stirred together in dry DCM (50 mL) under N₂ for 30 min. *N,N*-Diethylethylenediamine (0.22 mL, 1.87 mmol) was then added, and the mixture was stirred for a further 24 h at room temperature. Either the precipitated crude product was collected by filtration or solvent was removed by evaporation leaving crude product, which was taken up in 48% HBr (5 mL) and evaporated to dryness. Recrystallization from ethanol gave the hydrobromide salt as a white solid (0.41 g, 61%): mp 193.0–193.5 °C; ¹H NMR (DMSO) δ 9.39 (d, *J* = 1.2 Hz, 1H, 2-H), 9.18 (br s, 2H, N⁺H), 8.92 (br t, *J* = 5.9 Hz, 2H, CONH), 8.53 (¹/₂AB, *J* = 8.5 Hz, 4H, 2'-H, 6'-H), 8.11 (¹/₂AB, *J* = 8.5 Hz, 4H, 3'-H, 5'-H), 3.66 (m, 4H, CONHCH₂), 3.27 (br m, 12H, N⁺CH₂), 1.24 (t, *J* = 7.2 Hz, 12H, CH₂CH₃); ¹³C NMR (DMSO) 175.5 (C=O), 173.0 (C-4, C-6), 166.8 (C-2), 142.0 (C-1'), 137.6 (C-4'), 130.5 (C-3', C-5'), 130.4 (C-2', C-6'), 118.3 (C-5), 53.2 (CONHCH₂), 50.6 (N⁺CH₂CH₃), 37.6 (CONHCH₂CH₂), 10.8 (CH₃); IR (KBr) 3300m (NH), 1650s and 1540s (CONH), 1600s (Ar–CH), 1550s cm⁻¹; MS(CI) (free base) 517 (10%) (M + H)⁺, 221 ([PhCONH(CH₂)₂NEt₂]⁺, 15), 100 ([CH₂)₂NEt₂]⁺, 40), 86 ([CH₂NEt₂]⁺, 60), 74 (100), 44 (70). Hydrobromide salt: UV–vis (10 mM sodium phosphate buffer, pH 7.00, 1 mM EDTA, 300 mM NaCl) λ_{max} (nm) [ε (M⁻¹ cm⁻¹)] 255 [19 209], 291 [16 192]. Anal. (C₃₀H₄₀N₆O₂·2HBr·2H₂O) C, H, N.

4,6-Bis(4-[(2-(hydroxy)ethyl)carboxamido]phenyl)pyrimidine·0.5H₂O, 2c. Ester **3a** (0.5 g, 1.56 mmol) and ethanolamine (9 mL) were heated at 120 °C overnight under N₂. Evaporation of the excess ethanolamine left a pale-yellow residue, which was triturated twice with boiling chloroform, collected by filtration, and dried to give a white solid (0.46 g, 73%): mp 255–256 °C; ¹H NMR (DMSO) δ 9.36 (br s, 1H, 2-H), 8.77 (br s, 1H, 5-H), 8.67 (t, *J* = 5.0 Hz, 2H, exch D₂O, CONH), 8.49 (¹/₂AB, *J* = 8.0 Hz, 4H, 2'-H, 6'-H), 8.07 (¹/₂AB, *J* = 8.0 Hz, 4H, 3'-H, 5'-H), 4.82 (t, *J* = 5.0 Hz, 2H, OH), 3.54 (q, *J* = 5.0 Hz, 4H, CH₂O), 3.37 (q, *J* = 5.0 Hz, 4H, NCH₂); ¹³C NMR (DMSO) δ 165.7(C=O), 163.1 (C-4, C-6), 159.0 (C-2), 138.4 (C-4'), 136.7 (C-1'), 127.8 (C-2', C-6' or C-3', C-5'), 127.2 (C-3', C-5' or C-2', C-6'), 113.6 (C-5), 59.7 (OCH₂), 42.3 (NCH₂); IR (KBr) 3300s (OH, NH), 1650s and 1540s (CONH), 1600m (Ar–CH), 1260m, 1050m, 1025m cm⁻¹; HRMS (CI) found 407.1715 ([M + H]⁺), C₂₂H₂₃N₄O₂ requires 407.1715; MS (CI) (%) 407 ([M + H]⁺, 43), 389 ([M - OH]⁺, 7), 69 (100); UV–vis (10 mM sodium phosphate buffer, pH 7.00, 1 mM EDTA, 300 mM NaCl) λ_{max} (nm) [ε (M⁻¹ cm⁻¹)] 256 [16 454], 297 [17 162]. Anal. (C₂₂H₂₂N₄O₄·0.5H₂O) C, H, N.

Acknowledgment. This work was supported by the EPSRC (Grant GR/N 37605 to R.T.W. and T.C.J.), Yorkshire Cancer Research (program grant to T.C.J.), National Cancer Institute (Grant CA35635 to J.B.C.), and an EPSRC CASE studentship with Enact Pharma PLC.

Supporting Information Available: Figures and experimental information for rotational energy barrier determination; synthesis procedure for compounds **1b–f** and **2d–g**; table of calculated van't

Hoff enthalpies; telomerase assay data; list of nucleic acid structures used in the competition dialysis assay; table of competition dialysis data; elemental analysis data for all compounds. This material is available free of charge via the Internet at <http://pubs.acs.org>.

References

- Levine, M.; Tjian, R. Transcription Regulation and Animal Diversity. *Nature* **2003**, 147–151.
- Jenkins, T. C. Targeting Multi-Stranded DNA Structures. *Curr. Med. Chem.* **2000**, 7, 99–115.
- Arthanari, H.; Bolton, P. H. Functional and Dysfunctional Roles of Quadruplex DNA in Cells. *Chem. Biol.* **2001**, 8, 221–230.
- Mergny, J.-L.; Hélène, C. G-Quadruplex DNA: A Target for Drug Design. *Nat. Med.* **1998**, 4, 1366–1367.
- Ren, J.; Qu, X.; Dattagupta, N.; Chaires, J. B. Molecular Recognition of a RNA:DNA Hybrid Structure. *J. Am. Chem. Soc.* **2001**, 123, 6742–6743.
- Zaman, G. J.; Michiels, P. J.; van Boeckel, C. A. Targeting RNA: New Opportunities To Address Drugless Targets. *Drug Discovery Today* **2003**, 8, 297–306.
- Siddiqui-Jain, A.; Grand, C. L.; Bearss, D. J.; Hurley, L. H. Direct Evidence for a G-Quadruplex in a Promoter Region and Its Targeting with a Small Molecule To Repress c-MYC Transcription. *Proc. Nat. Acad. Sci. U.S.A.* **2002**, 99, 11593–11598.
- Grand, C. L.; Han, H.; Munoz, R. M.; Weitman, S.; Von Hoff, D. D.; Hurley, L. H.; Bearss, D. J. The Cationic Porphyrin TMPyP4 Down-Regulates c-MYC and Human Telomerase Reverse Transcriptase Expression and Inhibits Tumor Growth in Vivo. *Mol. Cancer Ther.* **2002**, 1, 565–573.
- Catasti, P.; Chen, X.; Moyzis, R. K.; Bradbury, E. M.; Gupta, G. Structure–Function Correlations of the Insulin-Linked Polymorphic Region. *J. Mol. Biol.* **1996**, 264, 534–545.
- Dai, J. X.; Dexheimer, T. S.; Chen, D.; Carver, M.; Ambrus, A.; Jones, R. A.; Yang, D. Z. An Intramolecular G-Quadruplex Structure with Mixed Parallel/Antiparallel G-Strands Formed in the Human BCL-2 Promoter Region in Solution. *J. Am. Chem. Soc.* **2006**, 128, 1096–1098.
- De Armond, R.; Wood, S.; Sun, D. Y.; Hurley, L. H.; Ebbinghaus, S. W. Evidence for the Presence of a Guanine Quadruplex Forming Region within a Polypurine Tract of the Hypoxia Inducible Factor 1 Alpha Promoter. *Biochemistry* **2005**, 44, 16341–16350.
- Sun, D. Y.; Guo, K. X.; Rusche, J. J.; Hurley, L. H. Facilitation of a Structural Transition in the Polypurine/Polypyrimidine Tract within the Proximal Promoter Region of the Human VEGF Gene by the Presence of Potassium and G-Quadruplex-Interactive Agents. *Nucleic Acids Res.* **2005**, 33, 6070–6080.
- Rankin, S.; Reszka, A. P.; Huppert, J.; Zloh, M.; Parkinson, G. N.; Todd, A. K.; Ladame, S.; Balasubramanian, S.; Neidle, S. Putative DNA Quadruplex Formation within the Human c-kit Oncogene. *J. Am. Chem. Soc.* **2005**, 127, 10584–10589.
- Todd, A. K.; Johnston, M.; Neidle, S. Highly Prevalent Putative Quadruplex Sequence Motifs in Human DNA. *Nucleic Acids Res.* **2005**, 33, 2901–2907.
- Huppert, J. L.; Balasubramanian, S. Prevalence of Quadruplexes in the Human Genome. *Nucleic Acids Res.* **2005**, 33, 2908–2916.
- Keniry, M. A. Quadruplex Structures in Nucleic Acids. *Biopolymers* **2000**, 56, 123–146.
- Perry, P. J.; Jenkins, T. C. DNA Tetraplex-Binding Drugs: Structure-Selective Targeting Is Critical for Antitumour Telomerase Inhibition. *Mini-Rev. Med. Chem.* **2001**, 1, 31–41.
- Murphy, P. M.; Phillips, V. A.; Jennings, S. A.; Garbett, N. C.; Chaires, J. B.; Jenkins, T. C.; Wheelhouse, R. T. Biarylpyrimidines: A New Class of Ligand for High-Order DNA Recognition. *Chem. Commun.* **2003**, 1160–1161.
- Wilson, W. D.; Strekowski, L.; Tanious, F. A.; Watson, R. A.; Mokrosz, J. L.; Strekowska, A.; Webster, G. D.; Neidle, S. Binding of Unfused Aromatic Cations to DNA. The Influence of Molecular Twist on Intercalation. *J. Am. Chem. Soc.* **1988**, 110, 8292–8299.
- Wang, Y.; Patel, D. J. Solution Structure of the Human Telomeric Repeat d[AG₃(T₂AG₃)₃] G-Tetraplex. *Structure* **1993**, 1, 263–282.
- Lane, A. N.; Jenkins, T. C. Structures and Properties of Multi-Stranded Nucleic Acids. *Curr. Org. Chem.* **2001**, 5, 845–870.
- Soyfer, V. N.; Potaman, V. N. *Triple-Helical Nucleic Acids*; Springer-Verlag: New York, 1996.
- Bredereck, H.; Gompper, R.; Morlock, G. Formamid-Reactionen, VIII. Eine Neue Pyrimidin-Synthese (Formamid-Reaktionen, VIII. A New Pyrimidine Synthesis). *Chem. Ber.* **1957**, 90, 942–951.
- Herbert, C. G.; Bass, R. G.; Watson, K. A.; Connell, J. W. Preparation of Poly(arylene ether pyrimidine)s by Aromatic Nucleophilic Substitution Reactions. *Macromol.* **1996**, 29, 7709–7716.
- Shi, D.-F.; Wheelhouse, R. T. A Novel, High-Yielding Synthesis of meso-Substituted Porphyrins. *Tetrahedron Lett.* **2002**, 43, 9341–9342.
- Shi, D.-F.; Wheelhouse, R. T.; Sun, D.; Hurley, L. H. Quadruplex-Interactive Agents as Telomerase Inhibitors: Synthesis of Porphyrins and Structure–Activity Relationship for the Inhibition of Telomerase. *J. Med. Chem.* **2001**, 44, 4509–4523.
- Murphy, P. M.; Jenkins, T. C.; Wheelhouse, R. T. Synthesis of Molecular Twist Compounds and Evaluation of Their Interactions with Higher-Order DNA Structures. *Br. J. Cancer* **2001**, 85, 92–92.
- Hughes, G.; Wang, C. S.; Batsanov, A. S.; Fern, M.; Frank, S.; Bryce, M. R.; Perepichka, I. F.; Monkman, A. P.; Lyons, B. P. New Pyrimidine- and Fluorene-Containing Oligo(arylene)s: Synthesis, Crystal Structures, Optoelectronic Properties and a Theoretical Study. *Org. Biomol. Chem.* **2003**, 1, 3069–3077.
- Saygili, N.; Batsanov, A. S.; Bryce, M. R. 5-Pyrimidylboronic acid and 2-Methoxy-5-pyrimidylboronic Acid: New Heteroarylpyrimidine Derivatives via Suzuki Cross-Coupling Reactions. *Org. Biomol. Chem.* **2004**, 2, 852–857.
- Wu, C. C.; Lin, Y. T.; Chiang, H. H.; Cho, T. Y.; Chen, C. W.; Wong, K. T.; Liao, Y. L.; Lee, G. H.; Peng, S. M. Highly Bright Blue Organic Light-Emitting Devices Using Spirofluorene-Cored Conjugated Compounds. *Appl. Phys. Lett.* **2002**, 81, 577–579.
- Schomaker, J. M.; Delia, T. J. Arylation of Halogenated Pyrimidines via a Suzuki Coupling Reaction. *J. Org. Chem.* **2001**, 66, 7125–7128.
- Wong, K. T.; Hung, T. S.; Lin, Y. T.; Wu, C. C.; Lee, G. H.; Peng, S. M.; Chou, C. H.; Su, Y. L. O. Suzuki Coupling Approach for the Synthesis of Phenylene–Pyrimidine Alternating Oligomers for Blue Light-Emitting Material. *Org. Lett.* **2002**, 4, 513–516.
- Boucher, E.; Simard, M.; Wuest, J. D. Use of Hydrogen Bonds To Control Molecular Aggregation. Behavior of Dipyrindones and Pyridone–Pyrimidones Designed To Form Cyclic Triplexes. *J. Org. Chem.* **1995**, 60, 1408–1412.
- Schroter, S.; Stock, C.; Bach, T. Regioselective Cross-Coupling Reactions of Multiple Halogenated Nitrogen-, Oxygen-, and Sulfur-Containing Heterocycles. *Tetrahedron* **2005**, 61, 2245–2267.
- Aldrich product data, www.sial.com.
- Testaferri, L.; Tingoli, M.; Tiecco, M. A Convenient Synthesis of Aromatic Thiols from Unactivated Aryl Halides. *Tetrahedron Lett.* **1980**, 21, 3099–3100.
- Testaferri, L.; Tiecco, M.; Tingoli, M.; Chianelli, D. Simple Synthesis of Aryl Alkyl Thioethers and of Aromatic Thiols from Unactivated Aryl Halides and Efficient Methods for Selective Dealkylation of Aryl Alkyl Ethers and Thioethers. *Synth. Commun.* **1983**, 13, 751–755.
- Blaszczak, A.; Elbing, M.; Mayor, M. Bromine Catalyzed Conversion of *S-tert*-Butyl Groups into Versatile and, for Self-Assembly Processes, Accessible, Acetyl-Protected Thiols. *Org. Biomol. Chem.* **2004**, 2, 2722–2724.
- Moore, C. G.; Porter, M. The Reaction of 2,4-Dinitrobenzenesulphenyl Chloride with Organic Monosulphides. *Tetrahedron* **1960**, 9, 58–64.
- Pastuszak, J. J.; Chimiak, A. *tert*-Butyl Group as Thiol Protection in Peptide-Synthesis. *J. Org. Chem.* **1981**, 46, 1868–1873.
- Quintela, J. M.; Peinador, C. A Ready One-Pot Preparation for 7-Oxa- (or thia)-3,4,6-triazabenz[*d,e*]anthracene and 7-Oxa-3,4,6,9-Tetraza-benz[*d,e*]anthracene Derivatives. *Tetrahedron* **1996**, 52, 10497–10506.
- McConaughie, A. W.; Jenkins, T. C. Novel Acridine–Triazines as Prototype Combilexins: Synthesis, DNA Binding, and Biological Activity. *J. Med. Chem.* **1995**, 38, 3488–3501.
- Haq, I.; Ladbury, J. E.; Chowdhry, B. Z.; Jenkins, T. C. Molecular Anchoring of Duplex and Triplex DNA by Disubstituted Anthracene-9,10-diones: Calorimetric, UV Melting, and Competition Dialysis Studies. *J. Am. Chem. Soc.* **1996**, 118, 10693–10701.
- Wilson, W. D.; Tanious, F. A.; Fernandez-Saiz, M.; Rigl, C. T. Evaluation of Drug–Nucleic Acid Interactions by Thermal Melting Curves. *Drug–DNA Interaction Protocols*; Humana Press Inc.: Totowa, NJ, 1997; pp 219–240.
- Ren, J. S.; Chaires, J. B. Sequence and Structural Selectivity of Nucleic Acid Binding Ligands. *Biochemistry* **1999**, 38, 16067–16075.
- Ren, J. S.; Chaires, J. B. Preferential Binding of 3,3′-Diethyloxadicarbonyanine to Triplex DNA. *J. Am. Chem. Soc.* **2000**, 122, 424–425.
- Ren, J. S.; Chaires, J. B. Rapid Screening of Structurally Selective Ligand Binding to Nucleic Acids. *Methods Enzymol.* **2001**, 340, 99–108.
- Chaires, J. B. Competition Dialysis: An Assay To Measure the Structural Selectivity of Drug–Nucleic Acid Interactions. *Curr. Med. Chem.: Anti-Cancer Agents* **2005**, 5, 339–352.

- (49) Chaires, J. B.; Ren, J.; Hamelberg, D.; Kumar, A.; Pandya, V.; Boykin, D. W.; Wilson, W. D. Structural Selectivity of Aromatic Diamidines. *J. Med. Chem.* **2004**, *47*, 5729–5742.
- (50) Chaires, J. B.; Ren, J.; Henary, M.; Zegrocka, O.; Bishop, G. R.; Strekowski, L. Triplex Selective 2-(2-Naphthyl)quinoline Compounds: Origins of Affinity and New Design Principles. *J. Am. Chem. Soc.* **2003**, *125*, 7272–7283.
- (51) Hurley, L. H.; Wheelhouse, R. T.; Sun, D.; Kerwin, S. M.; Salazar, M.; Fedoroff, O. Y.; Han, F. X.; Han, H.; Izbicka, E.; Von Hoff, D. D. G-Quadruplexes as Targets for Drug Design. *Pharmacol. Ther.* **2000**, *85*, 141–158.
- (52) Read, M.; Harrison, R. J.; Romagnoli, B.; Tanious, F. A.; Gowan, S. H.; Reszka, A. P.; Wilson, W. D.; Kelland, L. R.; Neidle, S. Structure-Based Design of Selective and Potent G Quadruplex-Mediated Telomerase Inhibitors. *Proc. Natl. Acad. Sci. U.S.A.* **2001**, *98*, 4844–4849.
- (53) Kim, N. W.; Piatyszek, A. M.; Prowse, K. R.; Harley, C. B.; West, M. D.; Ho, P. L. C.; Coviello, G. M.; Wright, W. E.; Weinrich, S. L.; Shay, J. W. Specific Association of Human Telomerase Activity with Immortal Cells and Cancer. *Science* **1994**, *266*, 2011–2015.
- (54) Wheelhouse, R. T.; Sun, D.; Han, H.; Han, F. X.; Hurley, L. H. Cationic Porphyrins as Telomerase Inhibitors: The Interaction of Tetra(*N*-methyl-4-pyridyl)porphine with Quadruplex DNA. *J. Am. Chem. Soc.* **1998**, *120*, 3261–3262.
- (55) Izbicka, E.; Wheelhouse, R. T.; Raymond, E.; Davidson, K. L.; Lawrence, R. A.; Sun, D.; Windle, B. E.; Hurley, L. H.; Von Hoff, D. D. Effects of Cationic Porphyrins as G-Quadruplex Interactive Agents in Human Tumour Cells. *Cancer Res.* **1999**, *59*, 639–644.
- (56) Fedorov, O. Y.; Salazar, M.; Han, H.; Chemeris, V. V.; Kerwin, S. M.; Hurley, L. H. NMR-Based Model of a Telomerase-Inhibiting Compound Bound to G-Quadruplex DNA. *Biochemistry* **1998**, *37*, 12367–12374.
- (57) Perry, P. J.; Jenkins, T. C. Recent Advances in the Development of Telomerase Inhibitors for the Treatment of Cancer. *Expert Opin. Invest. Drugs* **1999**, *8*, 1981–2008.
- (58) Perry, P. J.; Gowan, S. M.; Reszka, A. P.; Polucci, P.; Jenkins, T. C.; Kelland, L. R.; Neidle, S. 1,4- and 2,6-Disubstituted Amidoanthracene-9,10-dione Derivatives as Inhibitors of Human Telomerase. *J. Med. Chem.* **1998**, *41*, 3253–3260.
- (59) Jenkins, T. C. Optical Absorbance and Fluorescence Techniques for Measuring DNA–Drug Interactions. *Drug–DNA Interaction Protocols*; Humana Press Inc.: Totowa, NJ, 1997; pp 195–218.
- (60) Perrin, D. D.; Perrin, D. R.; Armarego, W. L. F. *Purification of Laboratory Chemicals*, 3rd ed.; Pergamon Press: Oxford, U.K., 1988.
- (61) Still, W. C.; Khan, M.; Mitra, A. Rapid Chromatographic Technique for Preparative Separations with Moderate Resolution. *J. Org. Chem.* **1978**, *43*, 2923–2925.

JM060315A